Nucleus-nucleus proximity potential and superheavy nuclei

W. D. Myers and W. J. Świątecki
Nuclear Science Division, Lawrence Berkeley National Laboratory, Berkeley, California 94720
(Received 13 April 2000; published 13 September 2000)

Using up-to-date values of nuclear radii and of the nuclear surface tension, the 1977 proximity treatment of nucleus-nucleus interaction is confronted with 113 measured fusion barriers. The $\approx 4\%$ overestimate of theory with respect to experiment, seen in a similiar comparison in 1981, is no longer present. The calculated proximity barriers, when applied to fusion reactions used to produce heavy elements with atomic number $Z=102-118$, suggest that the unexpectedly large cross section observed in the reaction $^{86}\mathrm{Kr}+^{208}\mathrm{Pb}\rightarrow^{293}118+1n$ may be due to the sinking of the Coulomb barrier below the level of the bombarding energy. Tests of this hypothesis are suggested. Some consequences of the appearance of such ''unshielded'' reactions for very heavy systems are discussed. An Appendix supplies very accurate analytic formulas for the universal nuclear proximity force and potential functions ϕ and Φ. This does away with the need to consult the tables published in 1977.

PACS number(s): 21.10.Dr, 25.70.Jj, 27.90.+b

I. INTRODUCTION

Knowledge of the nucleus-nucleus interaction potential is an essential ingredient in the analysis of elastic and inelastic scattering, as well as of fusion reactions between nuclei. In particular, information concerning this potential is necessary for interpreting and estimating cross sections for the synthesis of superheavy elements.

The proximity potential [1] provides a simple formula for the nucleus-nucleus interaction energy as a function of the separation between the surfaces of the approaching nuclei. The formula is free of adjustable parameters and makes use of the measured values of the nuclear surface tension and the surface diffuseness. However, in order to relate the separation between the nuclear surfaces to the distance between the centers of the approaching nuclei one needs, in addition, an accurate expression for the relevant nuclear radii (and, in the case of deformed nuclei, for other geometrical properties of the nuclear density distributions). In the early applications of the proximity potential to the calculation of fusion barriers, the surface energy was taken from [2], and the nuclear radii from a rough semiempirical formula [1], dating back to 1967 and 1977, respectively. In 1981 proximity barriers calculated in this way were compared with 96 measured fusion barriers for systems ranging from $^{9}\mathrm{Be}+^{10}\mathrm{B}$ to $^{40}\mathrm{Ar}+^{197}\mathrm{Au}$ [3]. The result was that the theory overestimated the measurements by about 4% on the average. For a parameterless theory this could be considered a success, but in practice a deviation of 4% for a barrier of the order of 200 MeV implies a significant deviation of 8 MeV.

In the past 25 years considerable progress has been made in the accurate determination of nuclear properties, including the surface energy coefficient [4] and nuclear radii [5]. Using such up-to-date values of nuclear parameters, the present paper reanalyzes the confrontation of the proximity barriers with the 1981 set of measurements in [3], as well as with more recent data. The result is that the 4% discrepancy between theory and measurement is no longer present.

In the second part of the paper (Sec. IV) we present an application of the proximity treatment to a discussion of recently measured cross sections for the synthesis of very heavy nuclei.

II. THE PROXIMITY POTENTIAL

For two approaching nuclei with atomic numbers Z_1 and Z_2 , center separation r and density distributions assumed spherical and frozen, the nucleus-nucleus interaction potential may be approximated as follows:

$$V(r)=\frac{Z_1Z_2e^2}{r}+K\Phi(\zeta) \quad \text{for } s>0. \tag{1}$$

Here e is the charge unit and ζ stands for s/b, where b is the (Süssmann) measure of the diffuseness of the nuclear surface [1], taken as 1 fm [4], and s is the separation between the half-density surfaces of the nuclei, given by

$$s=r-(C_1+C_2), \tag{2}$$

where C_1 and C_2 locate the half-density radii of the matter distributions of the two nuclei. (The most comprehensive measurements of nuclear sizes refer to *charge* radii, from which the matter radii have to be inferred. This may be done with the help of the droplet model, as described in Appendix A.) The dimensionless proximity potential function Φ, based on a Thomas-Fermi treatment of the nuclear surface, was tabulated in [1], and an analytic representation is given in Appendix B. The strength factor K is given by

$$K=4\pi\gamma Cb, \tag{3}$$

where C is the reduced radius defined by

$$C=C_1C_2/(C_1+C_2), \tag{4}$$

and where for γ we shall take the mean of the surface tension coefficients appropriate for the two nuclei (explicit expressions are provided in Appendix A).

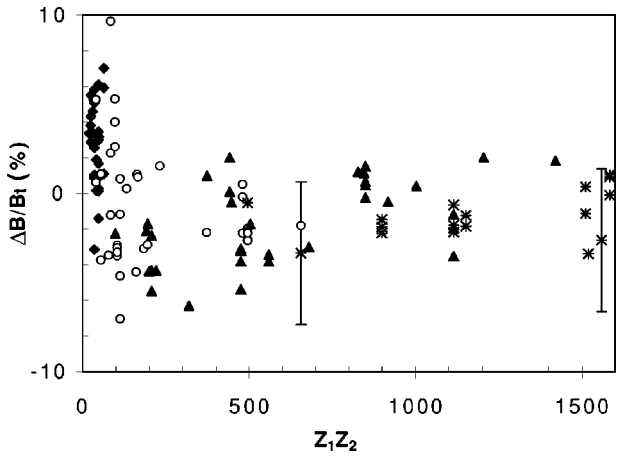

FIG. 1. The percentage deviations of experimental from calculated fusion barriers. Diamonds refer to a group of ''light'' reactions, circles to ''mixed'' reactions, and triangles to ''heavier'' reactions, all dating back to 1981 (see text). Stars refer to mean values of barrier distributions deduced from more recent measurements. The two vertical bar symbols indicate typical variances of such distributions.

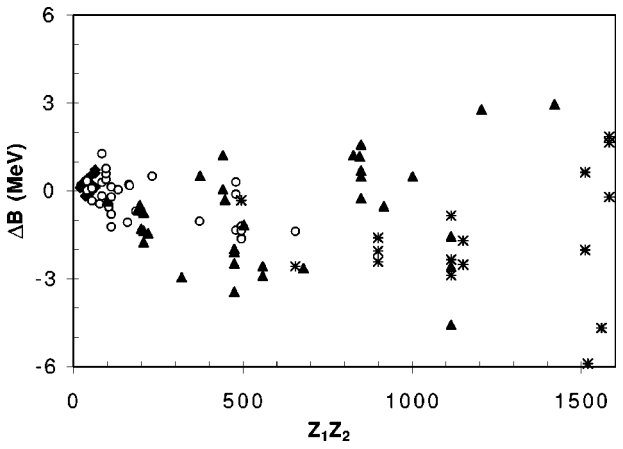

FIG. 2. The same data as in Fig. 1, but displayed as the actual rather than the percentage differences between experimental and calculated barriers.

In what follows we shall be concerned only with the case when $s>0$, where the electrostatic repulsion is given to an adequate approximation by $Z_1Z_2e^2/r$.

The maximum in the interaction potential is obtained from

$$-\frac{dV}{dr}=\frac{Z_1Z_2e^2}{r^2}+\frac{K}{b}\phi(\zeta)=0, \tag{5}$$

where ϕ, the proximity force function (the negative derivative of Φ with respect to ζ) is also tabulated in [1] and represented by a formula in Appendix B. Equations (1) and (5) define a nominal fusion barrier. It is ''nominal'' because it refers to frozen, spherical density distributions. Such barriers can serve as baseline estimates with respect to which one may discuss the effects of degrees of freedom other than the single approach variable r. These may include deformation and orientation degrees of freedom, changes in the nuclear density distributions, as well as effects of quantal fluctuations in these variables.

III. COMPARISON WITH MEASUREMENTS

Figure 1 displays, as a function of Z_1Z_2, the percentage deviations $(B_{exp}-B_{th})/B_{th}$ of 98 calculated barriers from the 96 measured values listed in [3]. (In one case there were three different calculations with slightly different radii assumed for the interacting nuclei—hence the extra two calculated entries.) Figure 1 may be compared with the bottom panel of Fig. 5 in [3], which displays the negative of $(B_{exp}-B_{th})/B_{exp}$ as a function of $\log Z_1Z_2$. The diamonds in Fig. 1 refer to a set of 29 ''light'' reactions with both Z_1 and $Z_2<9$, the circles to a set of 35 ''mixed'' reactions with either Z_1 or $Z_2<9$, and the triangles to a set of 34 ''heavier'' reactions with both Z_1 and $Z_2>8$. The average deviation for all 98 points is -0.01% to be compared with a deviation of about -4% according to Fig. 5 in [3]. The rms spread of the deviations in Fig. 1 is 3.30%. For the three separate groups of reactions the corresponding numbers are as follows: mean 2.74%, rms 3.64% (''light''); mean -0.68%, rms 3.37% (''mixed''); mean -1.66%, rms 2.89% (''heavier''). The stars in Fig. 1 refer to more recent data, ranging from ^{16}O $+^{144}$Sm to ^{86}Kr$+^{104}$Ru [6]. In those references the fusion data were analyzed not in terms of a single barrier, as in [3], but in terms of distributions of barrier heights. A star in Fig. 1 indicates the approximate mean of such a distribution. The variances of the distributions are typically 2% to 6% and a nominal value of 4% is indicated by a vertical bar attached to two of the stars in Fig. 1. (These are not experimental errors, but illustrations of typical variances of the distributions deduced from the analysis of the data.)

Figure 2 displays the actual values of $B_{exp}-B_{th}$ in MeV. For the 98 points (excluding the stars) the mean deviation is -0.35 MeV. For the three separate groups from ''light'' to ''heavier'' the corresponding numbers are 0.18 MeV, -0.34 MeV, and -0.80 MeV.

Figures 1 and 2 suggest the following conclusions. First, the systematic 4% overestimate of the measured values by the old proximity barriers is no longer present. This is the result of using accurate values of nuclear radii (either based on measurements [7] or on accurate systematics [5]) as well as the use of the nuclear surface energy coefficient given by the well-tested Thomas-Fermi model of [4]. (See Appendix A.) Thus, the one-degree-of-freedom proximity barriers provide a baseline close to measured values of fusion barriers. It is quite remarkable that even for the ''light'' reactions the observed barriers differ on the average by a mere 0.18 MeV (2.74%) from the values calculated using the proximity scheme, which formally is supposed to be accurate only for large nuclei, whose surface curvatures are small. (The ''light'' reactions include 5 cases where ^{4}He was the projectile.) But note that for the combined group of 49 ''heavier'' reactions (34 triangles and 15 of the 17 stars in Fig. 2) the experimental barriers are on average 1.07 MeV *below* the proximity baseline. This small difference may or may not be

significant in view of the uncertainties in the analysis of the data, but the implied trend in the deviations would not be unexpected as a possible effect of degrees of freedom other than *r*, whose presence is suggested by the observed widths of the barrier distributions.

On the whole, it is likely that displaying experimental data with respect to the nominal proximity barriers may throw light on the participation of additional degrees of freedom in fusion. One may also hope that the calculated barriers will prove to be a fair guide for estimating fusion barriers in cases where measurements do not exist.

IV. SUPERHEAVY NUCLEI

In this section we shall describe a recent application of the proximity potential to an examination of fusion cross-sections. The upper part of Fig. 3 (taken from [8]) shows the exponentially decreasing cross-sections for synthesizing heavy elements by bombarding ^{208}Pb and ^{209}Bi with progressively heavier projectiles, from ^{48}Ca, through ^{70}Zn to ^{86}Kr [9,10]. The bombarding energies were always such that the excitation energy of the compound nucleus was about 13 MeV which, up to ^{58}Fe+^{208}Pb, appears to be optimal for emitting just one neutron. (With projectiles heavier than ^{58}Fe excitation functions that would determine the optimum value of the excitation energy are fragmentary or nonexistent.) Note the break in the systematics of the cross sections in going from ^{70}Zn to ^{86}Kr. The thick curves in the lower part of Fig. 3 show the interaction potentials in the entrance channel—electrostatic (dashed curve) plus proximity—in relation to the bombarding energy, shown by the thick horizontal arrow. The potential energies are plotted against the overall extension of the reacting system, i.e., as a function of the distance between the outer tips of the approaching partners (assumed spherical) before contact, and as a function of the major axis of the fusing configuration after contact. Thus the medium weight vertical line corresponds to the diameter of a spherical compound nucleus, the thin vertical line to the contact of the half-density radii (''firm contact'') and the dashed vertical line to the contact of the density tails (''gentle contact''). The latter is where for the first time the fastest nucleons in the approaching nuclei can be exchanged without help from quantal penetration. At ''firm contact'' the slowest nucleons can be exchanged for the first time. According to a Thomas-Fermi model of the nuclear surface, ''gentle contact'' is about 2.74 fm outside ''firm contact'' [1]. The thick dashed curve is a free-hand interpolation of the entrance channel energy between firm contact and the spherical configuration. The medium weight curve is the macroscopic deformation energy along the fission valley in the absence of shell effects. (It is a liquid-drop estimate of the deformation energy along the ''y-family'' of saddle-point shapes—see [15].) The most important effect of shell structure is to produce a ground-state hollow (indicated by a diamond), which is guarded against fission by a barrier, whose position is shown by a square [11].

Figure 3 suggests a correlation between the break in the systematics of the measured cross-sections and the lowering of the Coulomb barrier ''shield'' which, for the lighter systems, guards the compound nucleus against a direct attack at the low energies designed to result in the emission of one neutron. At these energies it is quite remarkable that in the approach degree of freedom *r*, the lighter projectiles up to ^{70}Zn would be stopped already around gentle contact, where the tails of the nuclear densities are barely touching. The system is then faced with either relying on quantal penetration of the Coulomb barrier (which can drastically reduce the cross section), or avoiding the barrier by making use of a neck-growth degree of freedom. The danger with the latter is that this injects the system into the fission valley, whose bottom at the elongation corresponding to gentle contact is not only below the level of the saddle-point barrier guarding the compound-nucleus ground state, but also slopes *away* from that barrier, in the direction of fission. This is the physics of the entrance channel hindrance that goes by the name of ''extra push'' [9]. It is likely that this hindrance factor is contributing to the rapid decrease of the cross sections in Fig. 3 [9]. By contrast, once the Coulomb shield is out of the way, the system has a chance of proceeding for a time—at least to firm contact, if not beyond—along (or close to) the simple approach degree of freedom, avoiding the near-fatal growth of the neck. This will be the more likely the larger the stabilizing effects of the shell energy in the target and projectile: the shell energy resists neck growth because this extra binding is certain to be destroyed by a growing neck. In this connection it is interesting to note that the shape-dependent ''congruence energy'' of [12], related to the ''Wigner term'' in nuclear mass formulas, acts like a shell effect: it too resists the transformation of two nuclei into one, resulting from the growth of the neck. (The negative congruence energy is approximately halved after fusion.) As an illustration, in the reaction ^{70}Zn+^{208}Pb, the initial shell effects are 2.82 MeV and -13.41 MeV, respectively, and the change in congruence energy is from an initial value of -9.60 MeV (the sum of -5.49 MeV and -4.11 MeV for the projectile and target) to the final value of -4.42 MeV, for a total neck-resisting energy of $(-13.41+2.82-9.60+4.42)$ MeV$=-15.77$ MeV. (All the above estimates are based on [4].)

The reason why unshielded reactions in Fig. 3 make their appearance only with sufficiently heavy target-projectile combinations is quite elementary. The energy needed to deform a compound nucleus into two tangent fragments is resisted by the surface energy and favored by the Coulomb energy. Hence, the greater the charge on the compound nucleus, the lower the Coulomb barrier (as measured with reference to the ground-state energy). Above some critical charge the Coulomb barrier will sink below the ground-state energy (or this energy augmented by some constant, like the 13 MeV in the examples above). This happens first for deformation into two equal pieces, where the Coulomb energy relief is greatest. For even higher charges there opens up a range of fragment asymmetries for which unshielding takes place. (Negative shell effects in the fragments will enhance the unshielding by lowering the energy of the tangent configuration.)

Coming back to Fig. 3, is it really true that it is the unshielding in the ^{86}Kr+^{208}Pb reaction that is responsible for

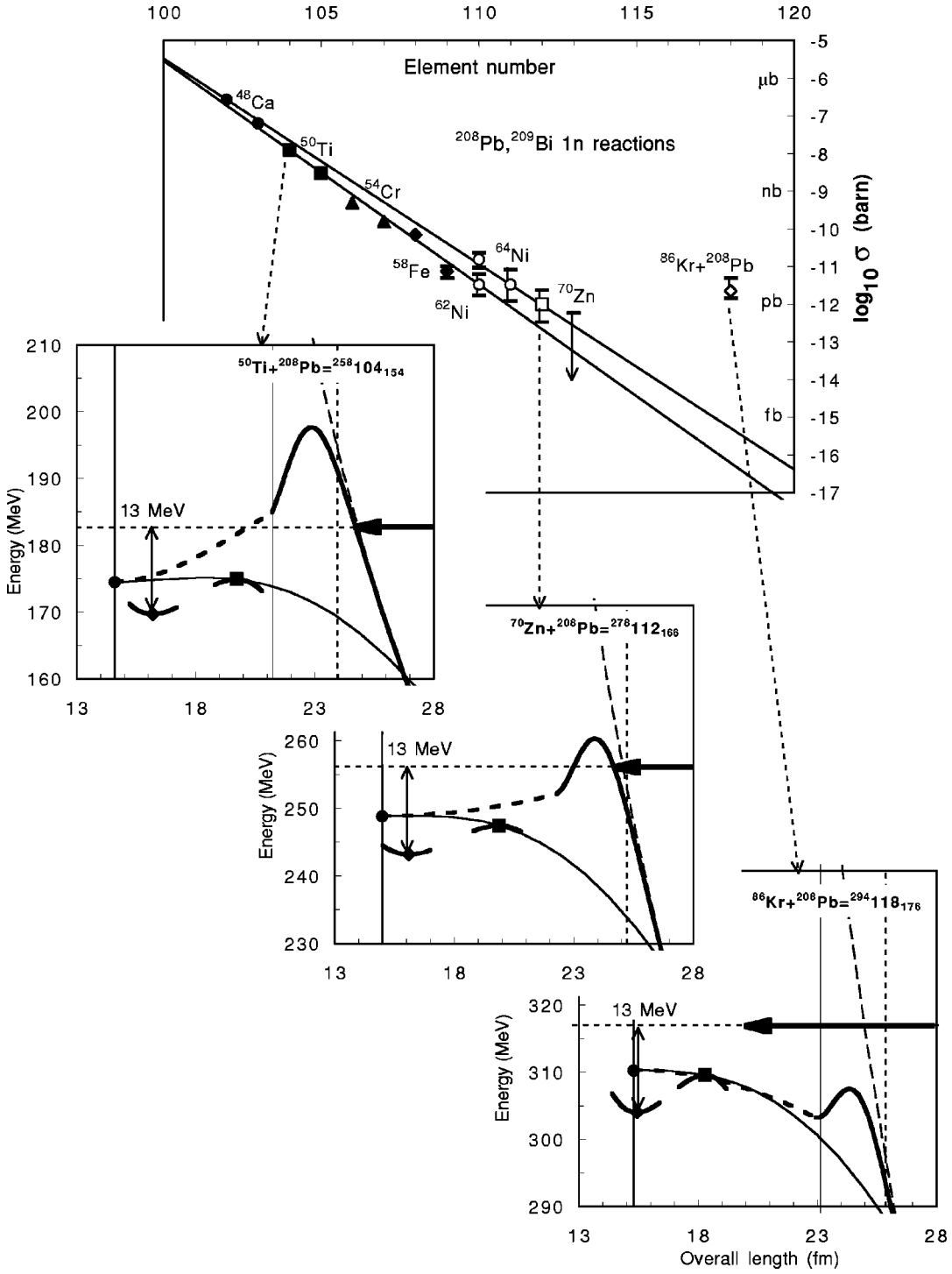

FIG. 3. The upper part refers to cross sections for synthesizing heavy elements from $Z=102$ to 118 in bombardments of ^{208}Pb and ^{209}Bi with projectiles from ^{48}Ca to ^{86}Kr. The lower part gives three examples of (center-of-mass) potential energy plots along the fusion valley (thick curves) and fission valley (thin curves). The plots are against the overall, tip-to-tip extension of the fusing or fissioning configuration. (See text for details.) Somewhere between the reactions Zn on Pb and Kr on Pb the Coulomb barrier dips below the bombarding energy, indicated by the thick horizontal arrow.

the enhancement of the corresponding cross-section by some four orders of magnitude with respect to a simple extrapolation? It is very difficult to be certain, and we must regard this interpretation as a tantalizing hypothesis that needs to be confirmed. But it turns out that it should not be too difficult to make an experimental test of this conjecture. Thus, element 112 was produced with a picobarn cross-section at the GSI laboratory in the shielded reaction ^{70}Zn+^{208}Pb $=^{278}112=^{277}112+1n$ [9]. The identical isotope can be reached in the unshielded reaction ^{136}Xe+^{142}Ce$=^{278}$112

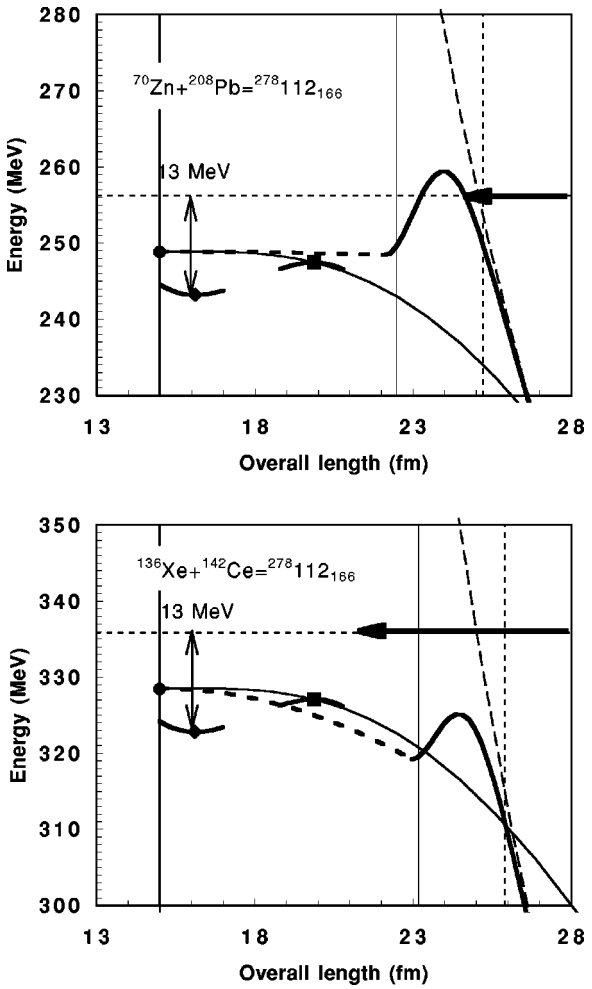

FIG. 4. This is like the lower part of Fig. 3. Here a comparison is made between a shielded and an unshielded reaction to make the same isotope of element 112, with the same excitation energy. (Note: In Fig. 4 the Coulomb barrier is a shade lower than in Fig. 3 because in the latter case an attempt was made to allow for the anticipated slight attenuation of the shell and congruence energies as the approaching nuclei begin to interact.)

$=^{277}112+1n$. Will the cross section be one or more orders of magnitude higher!? The two reactions are illustrated in Fig. 4. The compound nucleus is the same, the excitation is the same, the only difference is in the entrance channel. (It is also important to note that the neck-resisting shell and conguence energies are not very different: -15.77 MeV in the shielded reaction and -12.52 MeV in the proposed unshielded reaction.)

A similar test of the unshielding hypothesis would consist of comparing the shielded reaction ^{58}Fe+^{208}Pb=^{266}108 (which produced ^{265}108 with a peak cross section of about 70 picobarns [9]) with the unshielded reaction ^{128}Te+^{138}Ba $=^{266}$108. This comparison would be easier on account of the larger cross sections, but it is more ambiguous. This is because the neck-growth-resisting shell and congruence energies are rather different in the two cases: -19.06 MeV for the shielded reaction versus -11.22 Mev for the unshielded one, and this is expected to counteract the benefits of unshielding.

Unshielded reactions, if proved beneficial, would open a broad avenue for making several new elements and many new isotopes in the region of $Z>104$. In particular, the prospect for reaching the island of superheavy nuclei around $N=184$ and $Z=114$–126 would be much improved. Of the many fascinating candidate reactions, the unshielded combination ^{136}Xe+^{170}Er=$^{305}122+1n$ would be especially interesting, because its alpha decay products would overlap the decay chain of ^{289}114, suggested last year by the Dubna-Livermore collaboration as the result of the reaction ^{48}Ca $+^{244}$Pu=$^{289}114+3n$ [13]. These reactions may represent the closest approach to the predicted superheavy island centered at about $Z=114$, $N=182$ according to [11]. The ^{136}Xe $+^{170}$Er reaction has actually the advantage over the ^{48}Ca $+^{244}$Pu reaction of not using a rare projectile isotope and a radioactive target, and of being free of an alpha-decay background that may accompany transfer reactions on a heavy target. Also, if the island of stability turns out to be stretched or even shifted towards higher values of Z (for which there is some recent evidence [14]), then the Xe+Er reaction might be close to sampling the most stable part of such an island.

The above qualitative considerations, stimulated by the juxtaposition of the cross-section trends with proximity barriers in Fig. 3, suggest interesting perspectives for the future of heavy-element research. But it remains for the forthcoming experiments to decide on the feasibility of realizing these hopes.

ACKNOWLEDGMENTS

We would like to thank R. Smolańczuk for discussions and additional information on calculated shell effects and saddle-point shapes. We thank J. Wilczyński for advice concerning recent fusion barrier measurements. This work was supported in part by the Director, Office of Energy Research, Office of High Energy and Nuclear Physics, and by the Office of Basic Energy Sciences, Division of Nuclear Sciences, of the U.S. Department of Energy under Contract No. DE-AC03-76SF00098 and by the U.S.-Poland Maria Sklodowska-Curie Joint Fund II.

APPENDIX A

We used [7] to determine the half-density radii c either from the quoted ''two-parameter Fermi function'' fits or, in a few cases of light nuclei, from other parametrizations of the charge distributions. For nuclei not listed in [7] we had recourse to the accurate formulas from [5] representing the many measured rms values of the charge distributions, $\langle r^2\rangle^{1/2}$, expressed in terms of ''equivalent rms radii.'' These are denoted by R_{00} in [5] (and by Q in [15]) and are approximated in [5] by

$$R_{00}=\sqrt{5/3}\langle r^2\rangle^{1/2}=1.240A^{1/3}\left(1+\frac{1.646}{A}-0.191\frac{A-2Z}{A}\right)\text{fm}. \tag{A1}$$

To convert R_{00} to the half-density radius c we use the relation

$$c = R_{00}\left(1 - \frac{7}{2}\frac{b^2}{R_{00}^2} - \frac{49}{8}\frac{b^4}{R_{00}^4} + \cdots\right), \tag{A2}$$

obtained by eliminating the ''equivalent sharp radius'' R between Eqs. (4.17) in [15].

According to the droplet model [16] the matter radius C of a nucleus with N neutrons and Z protons is related to the charge radius c by

$$C = c + (N/A)t, \tag{A3}$$

where the neutron skin t is given by

$$t = \frac{3}{2}r_0\frac{JI - \frac{1}{12}c_1 ZA^{-1/3}}{Q + \frac{9}{4}JA^{-1/3}}. \tag{A4}$$

Here the radius constant r_0 has the value 1.14 fm, the symmetry energy coefficient J is equal to 32.65 MeV, $I=(N-Z)/A$, $c_1=(3/5)(e^2/r_0)=0.757895$ MeV and Q (not to be confused with the equivalent rms radius Q in [15]) is the neutron skin stiffness coefficient, equal to 35.4 MeV. (The values of all these nuclear parameters are taken from [4].)

Expressing the surface tension γ in terms of the surface energy coefficient a_2 defined by $a_2 = 4\pi r_0^2\gamma$, we may rewrite the strength factor K as

$$K = \frac{bCa_2}{r_0^2}. \tag{A5}$$

For a given nucleus, the value of a_2, including its dependence on neutron excess, is given by

$$a_2 = 18.63\ \text{MeV} - Q(t/r_0)^2. \tag{A6}$$

For a_2 in Eq. (A5) we shall take the average of the values appropriate to the two interacting nuclei, viz.

$$a_2 = 18.36\ \text{MeV} - Q(t_1^2 + t_2^2)/2r_0^2, \tag{A7}$$

where t_1 and t_2 are evaluated using Eq. (A4). [A subtle question concerns the sign of the second term in Eq. (A6), which depends on how one splits the total energy of a finite nucleus into a bulk term and a surface correction. In [17] these two versions of the surface tension coefficient are denoted by γ_e and γ_μ, and are given by Eqs. (78) and (79) and illustrated in Fig. 5 in that reference. For finite nuclei, either definition of the surface tension will give the correct total energy (the appropriate bulk term making up for the difference), but it can be shown [18] that only the version with the minus sign is truly associated with the surface region, and thus represents the nuclear surface tension that should be used in the proximity strength factor.]

APPENDIX B

The proximity functions $\phi(\zeta)$ and $\Phi(\zeta)$ tabulated in [1] may be represented as follows:

$$\phi(\zeta) = \sum_{i=0}^{5} c_n(2.5-\zeta)^n,$$

$$\Phi(\zeta) = -0.1353 + \sum_{i=0}^{5}\frac{c_n}{n+1}(2.5-\zeta)^{n+1} \quad \text{for} \quad 0<\zeta<2.5, \tag{B1}$$

$$\phi(\zeta) = -0.1331\exp\left[\frac{(2.75-\zeta)}{0.7176}\right],$$

$$\Phi(\zeta) = -0.09551\exp\left[\frac{(2.75-\zeta)}{0.7176}\right] \quad \text{for} \quad \zeta>2.5. \tag{B2}$$

The values of the constants c_n are as follows: $c_0=-0.1886$, $c_1=-0.2628$, $c_2=-0.15216$, $c_3=-0.04562$, $c_4=0.069136$, and $c_5=-0.011454$.

On the average, the above expressions reproduce the tabulated values to within about three units in the fourth decimal in the case of ϕ and better than that in the case of Φ. For $\zeta>2.74$ the exponential expressions are exact representations of the Thomas-Fermi calculations of the proximity functions [1].

[1] J. Blocki, J. Randrup, W.J. Świątecki, and C.F. Tsang, Ann. Phys. (N.Y.) **105**, 427 (1977).

[2] W.D. Myers and W.J. Świątecki, Ark. Fys. **36**, 343 (1967).

[3] L.C. Vaz, J.M. Alexander, and G.R. Satchler, Phys. Rep. **69**, 373 (1981).

[4] W.D. Myers and W.J. Świątecki, Nucl. Phys. **A601**, 141 (1996); Phys. Rev. C **60**, 014606 (1999).

[5] B. Nerlo-Pomorska and K. Pomorski, Z. Phys. A **348**, 169 (1994); B. Nerlo-Pomorska and B. Mach, At. Data Nucl. Data Tables **60**, 287 (1995).

[6] W. Reisdorf, F.P. Hessberger, K.D. Hildebrand, S. Hofmann, G. Münzenberg, K.-H. Schmidt, J.H.R. Schneider, W.F.W. Schneider, K. Sümmerer, G. Wirth, J.V. Kratz, and K. Schlitt, Nucl. Phys. **A438**, 212 (1985); W. Reisdorf, F.P. Hessberger, K.D. Hildebrand, S. Hofmann, G. Münzenberg, K.-H. Schmidt, W.F.W. Schneider, K. Sümmerer, G. Wirth, J.V. Kratz, K. Schlitt, and C.-C. Sahm, *ibid.* **A444**, 154 (1985); J.D. Bierman, P. Chan, J.F. Liang, M.P. Kelly, A.A. Sonzogni, and R. Vandenbosch, Phys. Rev. C **54**, 3068 (1996); N. Takigawa, K. Hagino, and S. Kuyucak, J. Phys. G **23**, 1367 (1997); M. Dasgupta, K. Hagino, C.R. Morton, D.J. Hinde, J.R. Leigh, N. Takigawa, H. Timmers, and J.O. Newton, *ibid.* **23**, 1491 (1997).

[7] C.W. de Jager, H. de Vries, and C. de Vries, At. Data Nucl. Data Tables **14**, 479 (1974); H. de Vries, C.W. de Jager, and C. de Vries, *ibid.* **36**, 495 (1987).

[8] W.D. Myers and W.J. Świątecki, ''The Dragon Guarding the Island of Superheavy Nuclei has dropped his Shield,'' talk presented at the Kasimir Grotowski Retirement Symposium, Kraków, Poland, 2000 [Acta Phys. Pol. B **31**, 1471 (2000)],

Lawrence Berkeley National Laboratory Report No. LBNL-45307, 2000.

[9] P. Armbruster, Rep. Prog. Phys. **62**, 465 (1999).

[10] V. Ninov, K.E. Gregorich, W. Loveland, A. Ghiorso, D.C. Hoffmann, D.M. Lee, H. Nitsche, W.J. Swiatecki, U.W. Kirbach, C.A. Laue, J.L. Adams, J.P. Patin, D.A. Shaughnessy, D.A. Strellis, and P.A. Wilk, Phys. Rev. Lett. **83**, 1104 (1999).

[11] R. Smolańczuk, Phys. Rev. C **56**, 812 (1997); and (private communications).

[12] W.D. Myers and W.J. Świątecki, Nucl. Phys. **A612**, 249 (1997).

[13] Yu.Ts. Oganessian, V.K. Utyonkov, Yu.V. Lobanov, F.Sh. Abdullin, A.N. Polyakov, I.V. Shirokovsky, Yu.S. Tsyganov, G.G. Gulbekian, S.L. Bogmolov, B.N. Gikal, A.N. Mezentsev, S. Iliev, V.G. Subbotin, A.M. Sukhov, G.V. Buklanov, K. Subotic, and M.G. Itkis, Phys. Rev. Lett. **83**, 3154 (1999).

[14] A.T. Kruppa, M. Bender, W. Nazarewicz, P.-G. Reinhard, T. Vertse, and S. Ćwiok, Phys. Rev. C **61**, 034313 (2000); M. Bender, *ibid.* **61**, 031302(R) (2000); Z. Patyk, I. Muntian, W.D. Myers, A. Sobiczewski, and W.J. Świątecki, Acta Phys. Pol. B **30**, 693 (1999).

[15] R.W. Hasse and W.D. Myers, *Geometrical Relationships of Macroscopic Nuclear Physics* (Springer-Verlag, Berlin, 1988).

[16] W.D. Myers and W.J. Świątecki, Ann. Phys. (N.Y.) **55**, 395 (1969); **84**, 186 (1974); Nucl. Phys. **A336**, 267 (1980).

[17] W.D. Myers, W.J. Świątecki, and C.S. Wang, Nucl. Phys. **A436**, 185 (1985).

[18] W.J. Świątecki, Lawrence Berkeley Laboratory Report No. 46753, 1999.